

# Kinetic studies of the reactions of O(<sup>1</sup>D) with several atmospheric molecules

Edward J. Dunlea<sup>ab</sup> and A. R. Ravishankara<sup>a</sup>

<sup>a</sup> Aeronomy Laboratory, National Oceanic and Atmospheric Administration, 325 Broadway, RAL 2, Boulder, CO 80305-3328, USA and The Department of Chemistry and Biochemistry and the Cooperative Institute for Research in Environmental Sciences, University of Colorado, Boulder, CO 80309, USA. E-mail: dunlea@post.harvard.edu; ravi@al.noaa.gov; Fax: 303-497-5822

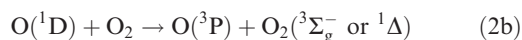
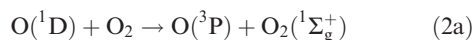
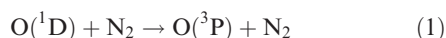
<sup>b</sup> Massachusetts Institute of Technology, 54-1320, 77 Massachusetts Avenue, Cambridge, MA 02139, USA. Tel: 617-253-2321

Received 8th January 2004, Accepted 25th February 2004  
First published as an Advance Article on the web 1st April 2004

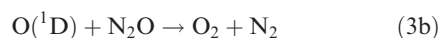
The rate coefficients for the removal of O(<sup>1</sup>D) by N<sub>2</sub>, O<sub>2</sub>, N<sub>2</sub>O, CO<sub>2</sub>, O<sub>3</sub> and n-butane were measured between 210 and 370 K. The appearance of O(<sup>3</sup>P) was observed following photolytic production of O(<sup>1</sup>D) in an excess of the reactants. The measured rate coefficients in this study, in units of 10<sup>-10</sup> cm<sup>3</sup> molecule<sup>-1</sup> s<sup>-1</sup>, are:  $k_1(\text{N}_2) = (0.195 \pm 0.020)\exp((125 \pm 20)/T)$ ;  $k_2(\text{O}_2) = (0.365 \pm 0.023)\exp((22 \pm 10)/T)$ ;  $k_3(\text{N}_2\text{O}) = (1.17 \pm 0.20)\exp((40 \pm 50)/T)$ ;  $k_4(\text{CO}_2) = (0.79 \pm 0.07)\exp((110 \pm 20)/T)$ ;  $k_5(\text{O}_3) = (2.65 \pm 0.35)\exp((-20 \pm 40)/T)$ ;  $k_6(\text{n-C}_4\text{H}_{10}) = (5.00 \pm 1.55)\exp((-10 \pm 90)/T)$ . The quoted uncertainties include estimated systematic errors and are at the 95% confidence level. Our results are compared with previous measurements, particularly the very recent data from Strekowski *et al.* (this issue) and Blitz *et al.*, (this issue), to produce a set of rate coefficients most appropriate for use in atmospheric calculations. The newly recommended rate coefficients, in units of 10<sup>-10</sup> cm<sup>3</sup> molecule<sup>-1</sup> s<sup>-1</sup>, are:  $k_1(\text{N}_2) = (0.21 \pm 0.02)\exp((115 \pm 10)/T)$ ;  $k_2(\text{O}_2) = (0.312 \pm 0.025)\exp((70 \pm 10)/T)$ ;  $k_3(\text{N}_2\text{O}) = (1.11 \pm 0.11)\exp((17 \pm 40)/T)$ ;  $k_4(\text{CO}_2) = (0.74 \pm 0.07)\exp((133 \pm 40)/T)$ ;  $k_5(\text{O}_3) = (2.37 \pm 0.36)\exp((6 \pm 15)/T)$ ;  $k_6(\text{n-C}_4\text{H}_{10}) = (5.35 \pm 0.54)\exp((-33 \pm 32)/T)$ .

## Introduction

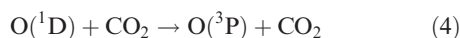
The reactions of the first electronically excited state of the oxygen atom (O(<sup>1</sup>D)) play a vital role in the chemistry of the atmosphere. O(<sup>1</sup>D) is produced in the troposphere and stratosphere mostly from the photolysis of O<sub>3</sub> by ultraviolet radiation. The majority of O(<sup>1</sup>D) is removed from the atmosphere by atmospheric gases, particularly molecular nitrogen and oxygen.



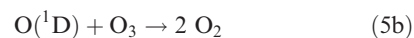
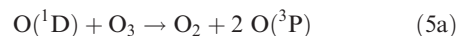
Yet O(<sup>1</sup>D) serves as the major source of two important reactive species, the hydroxyl (OH) in the troposphere and stratosphere *via* its reaction with H<sub>2</sub>O (and other H-containing species), and nitric oxide (NO) in the stratosphere through its reaction with N<sub>2</sub>O.<sup>1</sup>



The rate coefficients  $k_1$  and  $k_2$  along with the rate coefficient for the conversion of O(<sup>1</sup>D) to OH and  $k_3$ , are therefore critical in determining the rate of production of either OH or NO from O(<sup>1</sup>D). The rate coefficients for the removal of O(<sup>1</sup>D) by other gases are of importance for different reasons. The rate coefficient for the quenching of O(<sup>1</sup>D) by CO<sub>2</sub> is often measured in the laboratory for comparison with reactions (1) and (2):



Additionally, in the laboratory, O<sub>3</sub> photolysis is frequently used for the production of O(<sup>1</sup>D), requiring accurate knowledge of the rate coefficient for the reaction of O(<sup>1</sup>D) with O<sub>3</sub>:



Lastly, in another investigation,<sup>2</sup> the reaction of O(<sup>1</sup>D) with n-butane was used to produce OH *via* the reaction,



and OH detection was employed to trace the O(<sup>1</sup>D) temporal profile.

Current recommendations<sup>3,4</sup> of the rate coefficients for reactions (1)–(5),  $k_1$ – $k_5$ , have uncertainties as high as ±60% (corresponding to approximately two standard deviations; all uncertainties in this paper are reported at this 2σ level for consistency; IUPAC recommendations<sup>4</sup> are essentially the same as NASA/JPL,<sup>3</sup> only the latter is referenced from here on in this paper). There has been only one previous measurement of  $k_6$ .<sup>5</sup> The purpose of this study was to improve the accuracy of the measured values of these rate coefficients. We employed a pulsed photolysis–resonance fluorescence (PP–RF) apparatus for the detection of O(<sup>3</sup>P) to measure the rate coefficients for reactions (1)–(6) between 210 and 370 K. We discuss our results and compare them with previous measurements. A summary of the results on  $k_1$  from Georgia Tech, University of Leeds, and our laboratory was published in a previous paper.<sup>6</sup> The details of those results from our laboratory (which was not given in the previous publication) are also included in this paper, and the details from the other two groups are given in two other publications in this issue.<sup>2,7</sup>

## Experiments

The apparatus and experimental procedures were similar to those in our previous studies of  $O(^3P)$  or  $O(^1D)$  reactions.<sup>8,9</sup> Therefore, only the details essential for describing this study are given here.

A 250 cm<sup>3</sup> reactor, with a cross-sectional area of approximately 15.5 cm<sup>2</sup>, was temperature regulated (210 to 370 K,  $\pm 1$  K) by circulating cooled methanol or heated ethylene glycol through a jacket surrounding the reaction cell. The temperature of the gas flowing through the cell was measured with a calibrated chromel–alumel thermocouple. For all experiments, UHP He was used as the bath gas. Pressure in the reaction cell ranged from 5 to 50 Torr, as measured by a capacitance manometer (100 Torr). Total gas flow rates between 125 and 675 sccm were measured with calibrated electronic mass flow meters. The resulting linear flow velocities in the center of the reaction cell ranged from 10 to 30 cm s<sup>-1</sup>. This was the region where  $O(^1D)$  was produced and  $O(^3P)$  temporal profiles were measured.

$O(^3P)$  produced by  $O_3$  photolysis, reaction of  $O(^1D)$  with  $O_3$ , and quenching of  $O(^1D)$  was detected *via* the resonance fluorescence technique.<sup>8,9</sup> A continuous microwave discharge lamp was used for the detection of  $O(^3P)$  *via* VUV atomic resonance fluorescence near 130 nm. The microwave discharge lamp source consisted of a microwave cavity<sup>10,11</sup> surrounding a Pyrex flow tube that was  $\sim 1$  cm in diameter. The source gas for the plasma was UHP He at a pressure of  $\sim 2$  Torr and flowing rapidly through the tube. A solar blind photomultiplier tube, or PMT, (1.25" diameter alkali-halide photocathode capable of detecting 115 to 200 nm photons) that was positioned orthogonal to the microwave lamp and the laser beam, detected light primarily from the fluorescing  $O(^3P)$  atoms. The constant background signal due to scattered light from the discharge lamp reaching the PMT was measured (for  $\sim 2$  millisecond prior to  $O(^1D)$  production) and subtracted from the signal due to  $O(^3P)$ . Signal from the PMT was fed to a discriminator/pre-amplifier, and then into a digital counting board in a personal computer.

An entire temporal profile of  $O(^3P)$  was collected for each laser shot. The temporal profiles from hundreds to thousands of laser shots were added together to produce a temporal profile that could be fit to an analytical expression to describe the temporal variation of  $[O(^3P)]$  in the reaction cell (see Fig. 1). Each temporal profile was divided into a few thousand (3000–4000) time bins of 2 to 100  $\mu$ s width. The most precise rate coefficients were determined using widths of 2 to 10  $\mu$ s. We periodically examined the decay of  $O(^3P)$  signal at longer times using 75 or 100  $\mu$ s wide bins. In a separate experiment using a photodiode, it was determined that the laser pulse

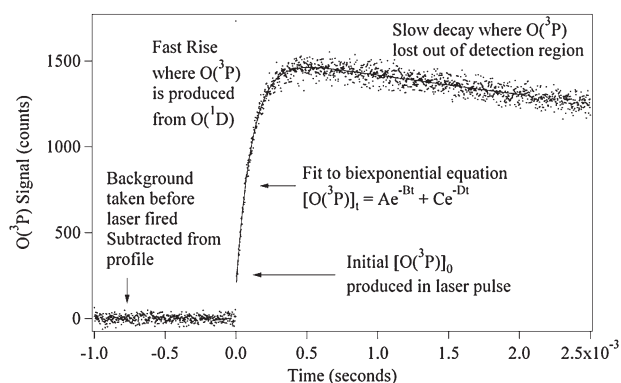
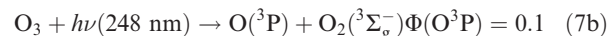
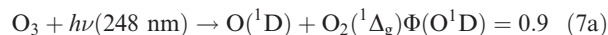


**Fig. 1** A typical temporal profile of the signal due to  $O(^3P)$  concentration following  $O_3$  photolysis at 248 nm in the presence of a reactant or quencher of  $O(^1D)$ . The amplitude of the signal provides information on how much  $O(^1D)$  is converted to  $O(^3P)$ .

arrived within 10 ns of the beginning of the first time bin, which we defined as time zero.

Ozone was photolyzed by a KrF excimer laser (peak wavelength = 248.4 nm,  $\Delta\lambda \sim 0.3$  nm, pulse width  $\sim 10$  ns) to produce  $O(^1D)$ . It is known that 248 nm photolysis of  $O_3$  produces both  $O(^1D)$  and  $O(^3P)$ :<sup>3,12,13</sup>

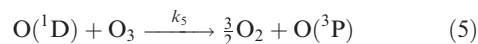
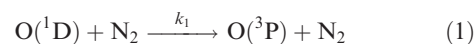


The fluence of the photolysis laser (0.4 to 10 mJ pulse cm<sup>-2</sup>, 0.5 cm<sup>2</sup> cross sectional area) was measured with a calibrated power meter after it exited the reactor. The concentration of  $O(^3P)$  was estimated from the amount initially produced by the laser, plus that created from the reaction of  $O(^1D)$  with  $O_3$  and from the quenching of  $O(^1D)$  by the reactant and/or the bath gas. Our resonance fluorescence signal varied linearly with  $O(^3P)$  concentration up to  $\sim 1 \times 10^{12}$  atom cm<sup>-3</sup>. We maintained  $O(^3P)$  concentrations well below this limit for all experiments. The detection sensitivity was  $2 \times 10^8$  atom cm<sup>-3</sup> (S/N  $\sim 1$  for 1 sec integration time).

Ozone was subjected to several freeze–pump–thaw cycles to remove  $O_2$  prior to making dilute mixtures of  $O_3$  in He ( $\sim 1\%$ ) in 12 L Pyrex bulbs. During all rate coefficient measurements, the  $O_3$  concentration in the gas stream flowing through the reactor was determined by measuring the absorption of 253.7 nm light ( $\sigma = 1.15 \times 10^{-17}$  cm<sup>2</sup>)<sup>3</sup> in a 100 cm long cell. The uncertainty in determining the  $O_3$  concentration, due to variation in the intensity of the light source, was estimated to be  $< \pm 2\%$ . The following gases (with the vendor and purity level indicated within parentheses) were used in these experiments without further purification: UHP He (US Welding,  $> 99.999\%$ ), UHP N<sub>2</sub> (Scott Specialty Gases,  $> 99.9995\%$ ), UHP O<sub>2</sub> (Scott Specialty Gases,  $> 99.99\%$ ), UHP CO<sub>2</sub> (Scott Specialty Gases,  $> 99.99\%$ ), N<sub>2</sub>O (Matheson Gases,  $> 99.99\%$ ), and n-butane (Aldrich,  $> 99\%$ ). Concentrations of these stable gases in the reactor were calculated using the measured mass flow rates and pressures. The uncertainties in the mass flow rate and pressure measurements were all  $\pm 2\%$ , leading to uncertainties of at most  $\pm 10\%$  ( $2\sigma$ ) for the concentration of the gases in the reactor. For the N<sub>2</sub> experiments, we used several different cylinders of UHP N<sub>2</sub> and UHP He to prepare dilute mixtures between 0.1–7%, some of which were then passed through a cold trap immersed in liquid nitrogen or an ethanol/dry ice mix. This eliminated any potential systematic errors due to the source of N<sub>2</sub>.

## Results

A typical  $O(^3P)$  temporal profile observed following the pulsed laser photolysis of  $O_3$  at 248 nm to produce  $O(^1D)$  is shown in Fig. 1. The following reactions took place following  $O(^1D)$  generation in the presence of N<sub>2</sub>, as an example, and account for the observed  $O(^3P)$  temporal profiles:



(Reaction (5) is a convenient representation of the process that has two sets of products,  $2 O(^3P) + O_2$  and  $2 O_2$ , but is equivalent to the reaction written above.)  $k_8$  is the rate coefficient for the loss of  $O(^3P)$  due to flow out of the detection region, which is the overlap of the laser beam and the microwave discharge lamp light,<sup>14</sup> and reactions with ozone and any impurities in

the bath gas.  $k_9$  is the rate coefficient for the removal of  $O(^1D)$  due to reaction with impurities in the bath gas and flow out of the detection region. The temporal profile of  $[O(^3P)]$  governed by these reactions is described by the equation:

$$[O(^3P)]_t = A e^{-Bt} + C e^{-Dt} \quad (I)$$

With  $N_2$  as the example reactant again, the parameters  $A$  to  $D$  are given by:

$$A = [O(^1D)]_0 \frac{(k_5[O_3] + k_1[N_2])}{(D - B)} \quad (II)$$

$$B = k_5 [O_3] + k_1 [N_2] + k_9 \quad (III)$$

$$C = [O(^3P)]_0 - A \quad (IV)$$

$$D = k_8 \quad (V)$$

The sum ( $A + C$ ) equals the initial  $O(^3P)$  concentration (in reality, the signal is proportional to the concentration) produced by photolysis. The first order rate coefficient for the rise (formation) of  $O(^3P)$  (the  $B$  parameter in eqn. (III)) equals the overall first order rate coefficient for the loss of  $O(^1D)$ . Thus, the addition of a reactant or quencher of  $O(^1D)$  increases the rate coefficient for the removal of  $O(^1D)$  and decreases the rise time of the  $O(^3P)$  signal.

We obtained  $O(^3P)$  temporal profiles at various concentrations of  $N_2$ ,  $O_2$ ,  $N_2O$ ,  $CO_2$  and *n*-butane at fixed concentrations of  $O_3$  to obtain the rate coefficients,  $k_1$  to  $k_4$  and  $k_6$ . In the case of reaction (5), the concentration of ozone was varied. Each measured  $O(^3P)$  profile was fit to eqn. (I) by a non-linear least squares method, described in more detail below. The slope of the plot of the first order rate coefficients for the  $O(^3P)$  rise versus the concentration of a reactant yielded the bimolecular rate coefficient for removal of  $O(^1D)$  by that species, *i.e.*, the sum of quenching to  $O(^3P)$  and reactive loss. The intercept of such a plot represented the sum of the first order rate coefficients for loss of  $O(^1D)$  due to reactions (5) and (9). In the case of  $O_3$ , the intercept (which was not measured) is the rate coefficient for the removal of  $O(^1D)$  via reaction (9) (see below). We kept these losses constant while we varied the concentration of the reactant. We measured the loss rate coefficient in the absence of reactant several times during the course of measuring  $k_1$  to  $k_4$  and  $k_6$ . Of course, such measurements were not possible while measuring  $k_5$  because ozone was both the reactant and the source of  $O(^1D)$ . The measured value of  $B$  in the absence of reactant was subtracted from the value of  $B$  measured with the reactant to obtain the first order rate coefficient for loss of  $O(^1D)$  due only to the reactant. We combine the results from different experiments, which employed various concentrations of  $O_3$  (Fig. 2). Experimental conditions, along with the obtained values of  $k_1$  to  $k_6$  are listed in Tables 1–6.

During the measurement of the rate coefficient for the reaction of  $O(^1D)$  with  $O_3$ , we determined  $k_9$  from the intercept of the plot of the first order rise rate coefficient (eqn. (III)) versus the concentration of  $O_3$ . This intercept was constant in a series of measurements where only the  $O_3$  concentrations were varied. In the bottom panel of Fig. 2, we combined the results from several room temperature experiments, each of which had a slightly different background loss rate coefficient, by subtracting  $k_9$  for that series from the individual first order rise rate coefficients. This background loss of  $O(^1D)$  in reaction (9) was mainly due to reaction with impurities in the bath gas, including any small air leaks into the reactor. Keeping this loss rate coefficient small (less than  $5000 \text{ s}^{-1}$ ) was important because the highest first order rate coefficient accurately measurable on our apparatus was only  $\sim 25\,000 \text{ s}^{-1}$ .

Early in this study, we investigated the robustness of the non-linear least squares fitting routine, in particular with respect to the number of parameters allowed to vary simultaneously and the fraction of the measured profile that was

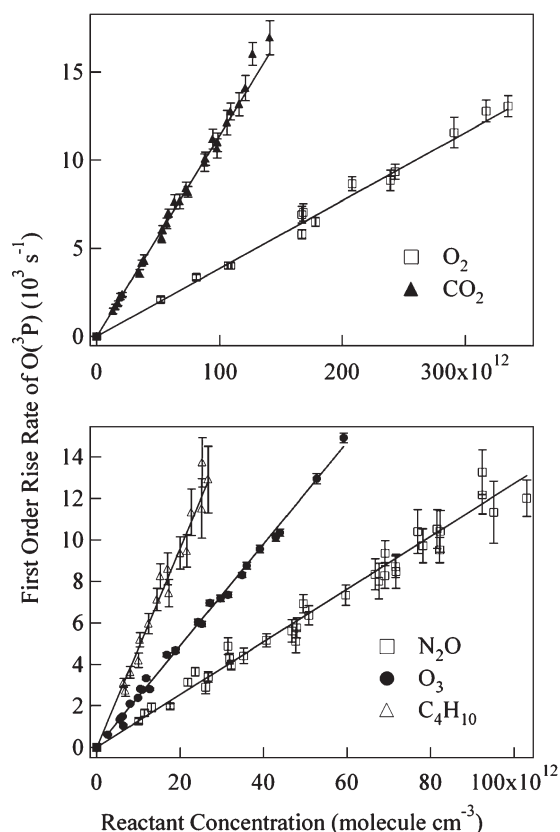


**Fig. 2** Plots of first order rise rate coefficients for the removal of  $O(^1D)$  versus the concentrations of  $O_2$  and  $CO_2$  (top panel) and concentrations of  $N_2O$ ,  $O_3$  and *n*- $C_4H_{10}$  (the bottom panel) at room temperature. The slope of each line is the bimolecular rate coefficient for removal of  $O(^1D)$  by that reactant, *via* both reaction and quenching.

used in the fit. Fitting the measured signal-versus-time profile while allowing all four parameters in eqn. (I) to vary could have led to values of  $A$ ,  $B$ ,  $C$  and  $D$  that were interdependent. Our procedure was to obtain the  $D$  parameter, the first order rate coefficient for the loss of  $O(^3P)$  via reaction (8), independently from a single exponential fit of the decaying portion of the temporal profile and then to use that value for the fit of the temporal profile to eqn. (I), allowing the other three parameters to vary.

The fitting routine automatically gave more weight to the larger signal values, *i.e.*, at the maximum  $O(^3P)$  concentration. Unfortunately, these signals are not as sensitive to the  $B$  parameter as the initial rapidly rising portion of the temporal profile. Therefore, we fit a small and constant proportion of the decaying portion of the curve (after the maximum in the  $O(^3P)$  concentration) in order to give it the same percentage weight in all profiles, rather than fitting a profile over the same number of points for all curves. The latter method would give the decaying portion of the curve a relatively larger weight for faster rises. The biexponential fits were carried out using data that covered roughly eight lifetimes for  $O(^1D)$  decay. Eight lifetimes included the rise of the signal to reach the maximum, the maximum in the signal, and a small portion of the signal decay, as shown in Fig. 1. Use of data covering six or ten lifetimes for the fit did not alter (*i.e.*, within the  $2\sigma$  uncertainty) the obtained value of the rise rate coefficient. Overall, we estimate an uncertainty of  $\pm 3\%$  in the first order rate coefficients for  $O(^1D)$  decay or  $O(^3P)$  rise attributable to the non-linear least squares fitting method and the choice of the range of data used here.

Overall, the  $2\sigma$  uncertainty in the measured values of the bimolecular rate coefficients reported at each temperature is

**Table 1** The measured values of  $k_1$  at 295 K and the experimental conditions employed for their determinations

$P/\text{Torr}$	Flow velocity/ $\text{cm s}^{-1}$	Repetition rate/Hz	$10^{-13}[\text{O}_3]/$ $\text{cm}^{-3}$	Fluence/ $\text{mJ pulse}^{-1} \text{cm}^{-2}$	$10^{-11}[\text{O}(^1\text{D})]_0/$ $\text{cm}^{-3}$	$10^{-13}[\text{N}_2]/$ $\text{cm}^{-3}$	$k_1'/\text{s}^{-1}$	$10^{11}k_1/$ $\text{cm}^3 \text{s}^{-1}$
11	15.2	2	2.04	1.1	3	7.20–24.0	7500–15 200	$3.27 \pm 0.49$
13.5	13.5	5	2.68	0.5	1.8	4.19–49.3	8100–23 500	$3.20 \pm 0.21$
13.5	13.5	5	2.15	0.5	1.4	3.85–44.4	6800–19 900	$2.76 \pm 0.33$
13.7	13.5	5	2.7	0.4	1.6	5.18–41.6	8200–20 400	$2.94 \pm 0.23$
14	13.2	5	2.46	0.5	1.6	2.56–43.0	7500–18 500	$3.10 \pm 0.13$
18.5	17.9	2.5	1	2.9	4	2.61–36.6	4100–17 300	$3.36 \pm 0.32$
18.5	17.9	2.5	0.96	2.8	3.6	11.6–42.4	3300–17 100	$3.22 \pm 0.25$
20	29.8	5	1.1	2	3	2.44–38.1	3700–17 300	$3.08 \pm 0.14$
15	29.7	4	1.1	3	4.4	3.50–23.9	4030–11 690	$3.22 \pm 0.12$
33	13.4	4	1.1	2.5	3.7	8.86–62.0	3950–20 600	$2.75 \pm 0.10$
33	13.5	4	0.9	2.5	3	5.69–58.0	3800–20 130	$2.81 \pm 0.12$
36	12.3	4	1.1	2	3	6.30–53.3	4750–19 820	$2.82 \pm 0.18$
33	13.4	4	1.1	2.5	3.7	6.93–36.6	4300–17 500	$3.00 \pm 0.35$
48	9.2	4	1.4	4.5	8.5	5.81–48.3	5700–19 380	$3.04 \pm 0.15$
22	17.2	4	1	3.5	4.7	3.28–34.3	4140–13 050	$2.77 \pm 0.16$
21	21.4	4	1.3	2–5	3–9	3.07–35.1	4100–13 750	$2.86 \pm 0.12$
18	23	4	1	3.5	4	2.30–42.4	3200–15 920	$2.94 \pm 0.11$
20	20.7	4	1.2	4.5	7	3.14–43.4	3290–15 310	$2.90 \pm 0.12$
23.5	17.6	4	1.2	5.5	8.1	5.65–50.9	4000–18 640	$2.98 \pm 0.16$
26	16.1	4	1.2	5	8	5.93–57.4	3900–21 600	$2.97 \pm 0.09$
30	14.1	4	1	3.5	7.5	4.23–45.5	3700–16 430	$2.86 \pm 0.26$
28	16.7	5	1.8	2	7	7.05–33.2	6000–18 050	$3.22 \pm 0.19$
27	15.7	5	1.9	2	8	6.93–42.1	6370–19 400	$3.22 \pm 0.34$
27	15.7	4	1.7	2	7	6.37–44.0	5805–19 500	$3.18 \pm 0.24$
10	16.8	10	0.7	2.4	2.3	5.93–25.0	5300–15 500	$3.43 \pm 0.29$
						Average <sup>a</sup>		$3.00 \pm 0.24$

<sup>a</sup> Including any estimated systematic errors.

a combination of the uncertainty in the slope of a plot of the first order rise rate coefficient *versus* the reactant concentration and the estimated systematic uncertainties in the measurements. The systematic uncertainties are due to the uncertainties in the concentration of the excess reagent ( $\text{N}_2$ ,  $\text{O}_2$ ,  $\text{CO}_2$ ,  $\text{O}_3$ ,  $\text{N}_2\text{O}$ , and n-butane) and possible systematic errors in the values of the first order rate coefficients derived using the non-linear least square fitting (and described earlier). If, for example, the first order rate coefficients were systematically overestimated by 5%, the derived value of the second order rate coefficient would also be 5% higher. However, the

fractional contribution could vary with the value of the rate coefficient. Therefore, we have opted merely include this as a possible systematic uncertainty.

We measured the rate coefficients for reactions (1)–(6) between 210 and 370 K; the obtained values are shown in Tables 1–7. A summary of our results on  $k_1$  were reported in recent letter,<sup>6</sup> along with the data from Georgia Tech. and the University of Leeds. Our results for  $k_2$  to  $k_6$  are plotted in Figs. 3–7 in the Arrhenius form:

$$\ln(k(T)) = \ln(A) - E_a/RT \quad (\text{VI})$$

**Table 2** The measured values of  $k_1$  at various temperatures and the experimental conditions employed for their determinations

$T/\text{K}$	$P/\text{Torr}$	Flow velocity/ $\text{cm s}^{-1}$	$10^{-13}[\text{O}_3]/$ $\text{cm}^{-3}$	Fluence/ $\text{mJ pulse}^{-1} \text{cm}^{-2}$ <sup>a</sup>	$10^{-11}[\text{O}(^1\text{D})]_0/$ $\text{cm}^{-3}$	$10^{-13}[\text{N}_2]/$ $\text{cm}^{-3}$	$k_1'/\text{s}^{-1}$	$10^{11}k_1/$ $\text{cm}^3 \text{s}^{-1}$
210	28	11.8	1	3.3	4.4	4.57–43.1	4100–21 350	$4.03 \pm 0.31$
210	35	8.8	1.2	3	8.5	5.91–54.8	5300–24 050	$3.25 \pm 0.29$
220	22	15.5	0.8	3	3.2	8.47–46.4	2720–20 060	$3.90 \pm 0.16$
230	34.5	9.8	1.3	3.5	9.5	8.31–59.9	5400–23 690	$3.05 \pm 0.20$
240	26	14.2	1.1	3	4.4	4.04–37.4	4650–18 830	$3.65 \pm 0.15$
250	25	15.8	1.05	2.6	3.7	7.70–57.0	5050–23 420	$3.45 \pm 0.28$
250	5.5	17	0.9	2	2.4	10.0–47.3	4120–21 220	$3.35 \pm 0.22$
250	34	10.7	1.1	3.5	8	3.63–56.7	4700–23 800	$3.05 \pm 0.27$
270	23	17.9	1.3	3	5.3	3.59–38.6	4100–16 740	$3.35 \pm 0.26$
270	33	11.9	1	3	7	5.10–60.7	4300–24 070	$2.93 \pm 0.19$
295		See Table 1						$3.00 \pm 0.24$
320	34	14.6	1.2	2.5	4	3.18–46.8	4000–19 000	$3.35 \pm 0.20$
320	33	13.9	0.9	3.5	7	4.98–56.5	3600–18 740	$2.73 \pm 0.12$
340	29	18.2	1.3	3	5.3	2.80–43.2	4500–18 110	$3.10 \pm 0.16$
340	36	13.6	7	3	5	4.94–61.8	3630–19 170	$2.50 \pm 0.08$
370	31	18.6	1.1	3	4.4	3.49–40.2	4100–15 650	$3.08 \pm 0.15$
370	35	15.2	0.8	3.5	5	2.83–53.2	3400–17 040	$2.52 \pm 0.14$

<sup>a</sup> Laser repetition rate between 4 and 5 Hz.

**Table 3** Measured values of  $k_2$  at various temperatures and the experimental conditions employed for their determinations

$T/K$	$P/\text{Torr}$	Flow velocity/ $\text{cm s}^{-1}$	$10^{-13}[\text{O}_3]/$ $\text{cm}^{-3}$	Fluence/mJ $\text{pulse}^{-1} \text{cm}^{-2a}$	$10^{-11}[\text{O}(^1\text{D})]_0/$ $\text{cm}^{-3}$	$10^{-13}[\text{O}_2]/$ $\text{cm}^{-3}$	$k_2'/\text{s}^{-1}$	$10^{11}k_2/$ $\text{cm}^3 \text{s}^{-1}$
220	28	11.3	0.52	3.75	4	4.88–46.1	3400–21 200	$4.15 \pm 0.37$
240	25	13.8	0.84–1.1	3	8	5.45–53.9	3200–19 900	$3.98 \pm 0.12$
265	19	20	1	3.75	9	2.34–43.9	4350–18 250	$4.09 \pm 0.27$
295	22	19.2	0.9	3	6	10.7–24.3	4300–12 000	$3.67 \pm 0.20$
295	22	19.2	0.78	3	5	17.8–33.5	4000–14 200	$3.86 \pm 0.24$
295	26	16.3	0.5	2.5–5	3–6	5.21–31.7	2200–14 300	$3.95 \pm 0.13$
320	26	17.7	0.5	3	3	3.92–56.5	4000–20 000	$4.06 \pm 0.30$
350	25	20.1	0.6	3	4	3.95–46.8	3750–17 700	$3.94 \pm 0.35$
370	25	21.2	0.76	2.8	4	4.24–45.0	3250–17 500	$3.70 \pm 0.22$

<sup>a</sup> Laser repetition rate 4 Hz.

where  $A$  is the pre-exponential factor,  $E_a$  is the activation energy of the reaction, and  $R$  is the universal gas constant. The precision in the Arrhenius pre-exponential factor was defined as

$$\sigma_A = A\sigma_{\ln(A)} \quad (\text{VII})$$

from the  $2\sigma$  precision of the linear least squares fit of eqn. (VI) to a straight line. The uncertainty in  $A$  shown in the tables also includes our estimated systematic error ( $\sim 8\%$ ) added in quadrature with the precision of the fits of  $k_1$  versus concentration plots.

## Discussion

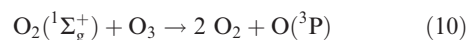
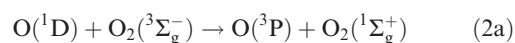
The kinetics of the atmospheric reactions of  $\text{O}(^1\text{D})$  has been studied since the early 1960's using a number of different techniques. Several studies<sup>15,16</sup> employed a resonance absorption technique to detect  $\text{O}(^1\text{D})$ , which has subsequently been shown to yield incorrect rate coefficients.<sup>3</sup> Other studies<sup>17–19</sup> have measured  $\text{O}(^1\text{D})$  rate coefficients using the resonance absorption of  $\text{O}(^3\text{P})$ . Still other studies<sup>20–24</sup> have observed the time

resolved fluorescence of  $\text{O}(^1\text{D}) \rightarrow \text{O}(^3\text{P})$  at 630 nm. And lastly, there have been a few previous studies<sup>9,25,26</sup> that employed resonance fluorescence detection of  $\text{O}(^3\text{P})$ , similar to the current investigation.

We have highlighted below the important previous determinations for the rate coefficients for reactions (2)–(6) in Tables 8–12. We discuss our results for the individual rate coefficients and compare them with the previous measurements. Our values of  $k_1$ , along with those from Strekowski *et al.*<sup>7</sup> and Blitz *et al.*<sup>2</sup> have been discussed elsewhere<sup>6</sup> and will not be repeated.

## $\text{O}_2$

The quenching of  $\text{O}(^1\text{D})$  by  $\text{O}_2$  produces electronically excited  $\text{O}_2(^1\Sigma_g^+)$ , and the subsequent reaction of  $\text{O}_2(^1\Sigma_g^+)$  with  $\text{O}_3$  also creates  $\text{O}(^3\text{P})$ .

**Table 4** The measured values of  $k_3$  at various temperatures and the experimental conditions employed for their determinations

$T/K$	$P/\text{Torr}$	Flow velocity/ $\text{cm s}^{-1}$	$10^{-13}[\text{O}_3]/$ $\text{cm}^{-3}$	Fluence/mJ $\text{pulse}^{-1} \text{cm}^{-2a}$	$10^{-11}[\text{O}(^1\text{D})]_0/$ $\text{cm}^{-3}$	$10^{-13}[\text{N}_2\text{O}]/$ $\text{cm}^{-3}$	$k_3'/\text{s}^{-1}$	$10^{10}k_3/$ $\text{cm}^3 \text{s}^{-1}$
295	32	15.0	1.30	0.5–1.2	3–8	1.98–12.6	5650–21 880	$1.20 \pm 0.15$
295	40	10	1.10	6.0	8.0	1.51–12.7	5500–21 250	$1.14 \pm 0.07$
295	22	17.0	0.93	3.5	4.4	1.09–5.49	4150–10 360	$1.01 \pm 0.10$
295	20	25.0	1.20	3.0–9.0	5–14	1.76–9.85	4100–15 180	$1.16 \pm 0.05$
295	26	16.5	1.48	2.1	8.0	1.31–9.51	6200–17 300	$1.25 \pm 0.11$
250	20	18.1	1.50	1.7	5.3	1.27–7.93	5500–18 000	$1.41 \pm 0.15$
220	20	16.0	1.55	1.7	6.0	1.12–8.26	6000–18 000	$1.49 \pm 0.08$
265	22	17.5	1.47	1.4	5.0	1.16–7.57	5500–16 150	$1.31 \pm 0.14$
295	19	22.5	0.97	2.6	5.0	0.99–6.76	4300–12 300	$1.24 \pm 0.03$
345	21	23.8	0.85	2.75	5.0	1.15–7.30	4000–13 200	$1.19 \pm 0.07$
370	23	23.3	1.09	3.3	8.0	1.19–7.28	4000–13 300	$1.28 \pm 0.06$
320	25	18.6	1.01	2.75	6.0	1.11–7.00	4600–13 300	$1.36 \pm 0.09$
280	25	16.2	1.22	3	9.0	1.42–8.55	5300–18 600	$1.45 \pm 0.10$
295	19	24.8	1.71	2.15	8.3	2.36–9.24	6600–18 500	$1.36 \pm 0.11$
295	20	22.1	1.77	2.0	8.2	2.18–10.3	5800–19 400	$1.30 \pm 0.13$
265	22	18.0	1.72	1.6	6.0	2.05–10.8	6700–20 500	$1.36 \pm 0.09$
235	20	17.6	1.83	1.5	6.0	1.03–8.16	6500–19 500	$1.35 \pm 0.08$
220	21	15.7	1.94	1.4	6.0	2.13–9.26	6850–16 900	$1.27 \pm 0.11$
250	21	17.8	1.48	1.65	6.0	1.22–9.29	6050–17 100	$1.43 \pm 0.13$
280	21	19.9	1.39	1.75	5.0	1.57–8.33	5500–16 700	$1.46 \pm 0.10$
295	21	21.0	1.50	1.9	6.0	1.14–9.24	5300–18 400	$1.34 \pm 0.13$
320	19	25.2	1.03	1.9	4.0	1.12–8.58	4400–16 300	$1.40 \pm 0.11$
370	20	27.7	1.02	2.15	5.0	1.83–7.44	4100–14 600	$1.31 \pm 0.14$
345	21	24.6	0.98	2.3	5.0	1.27–8.02	4400–16 500	$1.37 \pm 0.09$

<sup>a</sup> Laser repetition rate 4 Hz.

**Table 5** Measured values of  $k_4$  at various temperatures and the experimental conditions employed for their determinations

$T/K$	$P/\text{Torr}$	Flow velocity/ $\text{cm s}^{-1}$	$10^{-13}[\text{O}_3]/$ $\text{cm}^{-3}$	Fluence/ $\text{mJ pulse}^{-1} \text{cm}^{-2a}$	$10^{-11}[\text{O}(^1\text{D})]/$ $\text{cm}^{-3}$	$10^{-13}[\text{CO}_2]/$ $\text{cm}^{-3}$	$k_4'/\text{s}^{-1}$	$10^{10}k_4/$ $\text{cm}^3 \text{s}^{-1}$
220	20	15	1.17	2.4	6	1.44–12.4	6000–20 100	$1.29 \pm 0.09$
240	21	15.4	1.07	2.5	6	1.33–9.4	5800–17 100	$1.21 \pm 0.04$
260	23	15.2	1.41	2.5	8	1.58–9.78	6500–18 900	$1.26 \pm 0.03$
260	20	19	1.12	2.4	6	1.48–12.7	4600–20 300	$1.23 \pm 0.04$
280	20	19.3	0.86	2.5	5	1.37–11.8	4800–19 400	$1.18 \pm 0.01$
295	21	19.5	1.17	2.8	7	1.15–14.1	5200–20 800	$1.11 \pm 0.04$
295	20	19.6	1.08	2.9	7	1.33–9.44	5400–17 100	$1.18 \pm 0.04$
295	25	16.2	1.25	2.9	8	1.75–8.14	5000–16 600	$1.12 \pm 0.02$
295	18	22.3	0.94	2.75	6	1.93–10.6	5500–18 100	$1.14 \pm 0.01$
295	21	20.6	1.07	2.7	7	2.10–13.7	4400–21 300	$1.18 \pm 0.04$
295	22	22	1.35	4.3	7.7	0.70–8.79	4150–13 640	$1.13 \pm 0.08$
320	17	28.1	0.74	2.9	5	0.78–12.1	3400–18 000	$1.15 \pm 0.04$
345	20	25.8	0.61	2.9	4	0.84–12.5	3400–18 500	$1.12 \pm 0.05$
370	21	26.3	0.7	3	5	0.94–11.9	3900–17 100	$1.05 \pm 0.06$

<sup>a</sup> Laser repetition rate 4 Hz.

Therefore, care has to be exercised in minimizing the concentration of  $\text{O}_3$  in measuring  $k_2$ . We maintained the  $\text{O}_3$  concentration well below  $1 \times 10^{13}$  molecule  $\text{cm}^{-3}$ . Numerical simulations of the reactions governing the temporal profiles of  $\text{O}(^3\text{P})$  under our typical experimental conditions showed that the influence of reaction (10) on our measured rate coefficient was less than 1%.

Our result for the room temperature value of  $k_2$  agrees, within the error bars, with the current recommendation of  $(4.0 \pm 1.6) \times 10^{-11}$   $\text{cm}^3$  molecule $^{-1}$   $\text{s}^{-1}$ , which was based on the average of the three previous studies listed in Table 8 (uncertainties are reported at the  $2\sigma$  level). It is also in excellent agreement with the recent results of Strekowski *et al.* and Blitz *et al.* The reported values of  $k_2$  at 295 K range from  $3.67 \times 10^{-11}$  to  $4.2 \times 10^{-11}$   $\text{cm}^3$  molecule $^{-1}$   $\text{s}^{-1}$ , an exceedingly small range. The average of these values is  $k_2(295 \text{ K}) = 3.95 \times 10^{-11}$   $\text{cm}^3$  molecule $^{-1}$   $\text{s}^{-1}$ , because of the very small variation of  $k_2$  with temperature,  $k_2(298 \text{ K})$  is also  $3.95 \times 10^{-11}$   $\text{cm}^3$  molecule $^{-1}$   $\text{s}^{-1}$ . We assign an uncertainty of 15% at the  $2\sigma$  level to  $k_2(298 \text{ K})$ ; *i.e.*,  $f(298 \text{ K}) = 1.08$  in the terminology used in data evaluations. (The same notation is used for all the recommendations in this paper.)

The range of values for  $E_a/R$  from the four temperature-dependent studies listed in Table 8 is between  $-20$  and  $-90$ . The combined value of  $E_a/R$  from this study, Strekowski *et al.*,<sup>7</sup> and the previous study of Streit *et al.*<sup>22</sup> is  $(-70 \pm 10)$  K, as shown in Fig. 3 where values of  $k_2$ , normalized to a  $k_2(298 \text{ K}) = 4.0 \times 10^{-11}$   $\text{cm}^3$  molecule $^{-1}$   $\text{s}^{-1}$ , are plotted

against the reciprocal of temperature. We note that the value reported by Blitz *et al.* at 195 K is in excellent agreement with this value of  $E/R$ . The figure also shows the previously recommended value of  $k_2$ , which is essentially the same. We have plotted the range of values encompassed by  $A$ ,  $E/R$ , and  $k_2(298 \text{ K})$  derived by combining the available data. This derived value is also shown in Table 8.

## $\text{N}_2\text{O}$

Our result for the overall rate coefficient for reaction (3),  $k_3 = (1.27 \pm 0.08) \times 10^{-10}$   $\text{cm}^3$  molecule $^{-1}$   $\text{s}^{-1}$ , at room temperature is slightly higher than the current recommendation of  $(1.16 \pm 0.70) \times 10^{-10}$   $\text{cm}^3$  molecule $^{-1}$   $\text{s}^{-1}$ , but agrees within the quoted error bars. It is, however, roughly 20% larger than the value reported by Blitz *et al.* The range of room temperature values of  $k_3$  for the five studies listed in Table 9 is from 1.07 to 1.27 (in units of  $10^{-10}$   $\text{cm}^3$  molecule $^{-1}$   $\text{s}^{-1}$ ), which is a small range. Just like for  $k_2$ , we determined the average of the room temperature values of  $k_3$ ,  $k_3(298 \text{ K}) = (1.18 \pm 0.15) \times 10^{-10}$   $\text{cm}^3$  molecule $^{-1}$   $\text{s}^{-1}$ , then we normalized the temperature dependent data from this work, the one previous study<sup>21</sup> and the recent investigation of Blitz *et al.*<sup>2</sup> to obtain the temperature dependence reported in the table. None of three recent studies show significant temperature dependence for reaction (3) (see Fig. 4).

In addition to the studies listed in Table 9, one of more thorough tests of the accuracy of previous  $\text{O}(^1\text{D})$  reaction rate

**Table 6** Measured values of  $k_5$  at various temperatures and the experimental conditions employed for their determination

$T/K$	$P/\text{Torr}$	Flow velocity/ $\text{cm s}^{-1}$	$10^{-13}[\text{O}_3]/$ $\text{cm}^{-3}$	Fluence/ $\text{mJ pulse}^{-1} \text{cm}^{-2a}$	$10^{11}[\text{O}(^1\text{D})]/$ $\text{cm}^{-3}$	$k_5'/\text{s}^{-1}$	$10^{10}k_5/$ $\text{cm}^3 \text{s}^{-1}$
210	25	14	0.5–10.4	0.33–5.56	8.6	1580–14 970	$2.45 \pm 0.25$
220	19	19	0.4–1.7	0.50–6.67	6.4	1030–16 540	$2.48 \pm 0.12$
240	24	15.5	0.8–3.1	0.70–5.11	7.0	3410–14 870	$2.45 \pm 0.27$
250	22	17.7	0.5–2.0	0.64–5.26	3.5	2720–14 300	$2.37 \pm 0.27$
270	21	18.5	0.8–3.8	0.71–5.27	7.0	2580–13 620	$2.33 \pm 0.15$
295	22	20.0	0.9	0.96–4.96	1.0	2050–10 840	$2.37 \pm 0.24$
295	18	18.0	1.2–4.0	0.09–5.92	9.6	2060–16 000	$2.47 \pm 0.19$
295	20	36.5	1.6–3.8	0.55–3.48	7.5	1630–8860	$2.52 \pm 0.17$
295	18	25	1.5–9	0.62–3.91	8.80	2810–11 670	$2.38 \pm 0.01$
320	33	15	2.0–2.5	0.96–5.41	5.2	3440–14 340	$2.47 \pm 0.20$
340	30	20	0.5–10.9	0.49–7.26	7.2	1240–14 770	$2.68 \pm 0.16$
370	31	19	0.8–3.0	0.80–4.93	6.1	2860–13 310	$2.51 \pm 1.30$

<sup>a</sup> Laser repetition rate between 2.5 and 5 Hz.

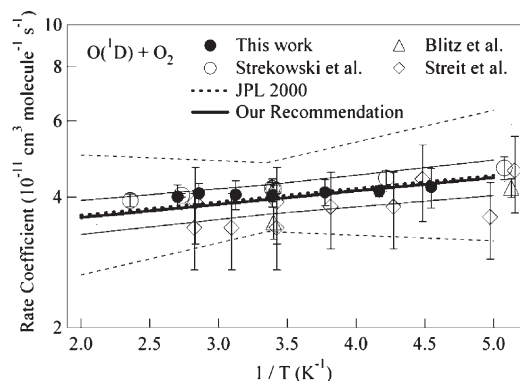


**Fig. 3** Arrhenius plot for reaction (2) showing  $k_2$  (on a logarithmic scale) against the inverse of the temperature. Previous temperature dependent studies from Table 8 are shown along with the results from this study and the new recommendation. Thick lines represent recommendations and the thin lines represent upper and lower error limits. See text for description of how the recommendation was determined.

coefficient measurements was the integrated experiment of Greenblatt and Ravishankara.<sup>27</sup> Using a chemiluminescence detector to measure the concentration of NO, they predicted the yield of NO from the photolytic production of  $O(^1D)$  in the presence of  $N_2$ ,  $O_2$  and  $CO_2$  based on the known values of the rate coefficients involved and constrained the value of  $k_3$  relative to  $k_1$ ,  $k_2$ , and  $k_4$ . By measuring only one species, *i.e.*, NO, in all experiments, they reduced the uncertainties associated with an absolute measurement of the NO yield. They assumed that all  $O(^1D)$  interactions, except for reaction (3), produced one  $O(^3P)$  per  $O(^1D)$ . This experiment reduced the uncertainty in the overall  $NO_x$  production rate from near 80% to less than 30%.

In light of our newer measurements of the rate coefficients involved in that experiment, we have re-analyzed the data of Greenblatt and Ravishankara. They had three sets of experiments: one with  $N_2O$  photolysis in the presence of  $N_2$  and  $O_2$  only, one with  $N_2O$  photolysis in the presence of  $N_2$ ,  $O_2$  and  $CO_2$ , and one with  $O_3$  photolysis at 248 nm in the presence of  $N_2$  and  $O_2$ . The average ratios of the measured yield of NO to the predicted yield of NO, using the recommended values of  $k_1$  to  $k_4$ , were 0.98, 1.30 and 1.09, respectively for the three experimental conditions. If we use the rate coefficients reported here, the same ratios are calculated to be 1.02, 1.23, and 1.13, which are all within the quoted error bars of the original ratios. The slight increase in the first and third ratios was the result of the slight increase in the rate coefficient for  $O(^1D) + N_2$  relative to that for  $O(^1D) + N_2O$  in using our more recent rate coefficients. The decrease in the second

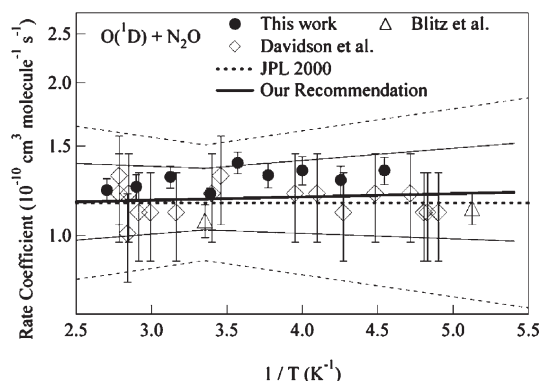


**Fig. 4** Arrhenius plot for reaction (3) showing  $k_3$  (on a logarithmic scale) against the inverse of the temperature. Previous temperature dependent studies from Table 9 are shown along with the results from this study and the new recommendation. Thick lines represent recommendations and the thin lines represent upper and lower error limits.

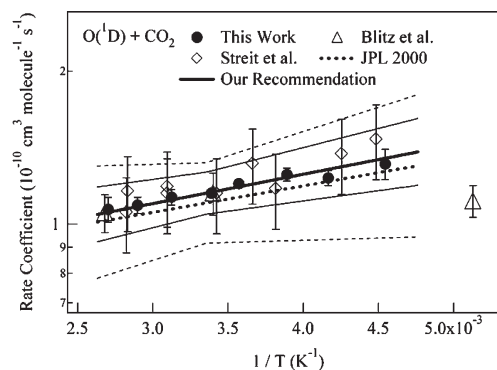


**Fig. 5** Arrhenius plot for reaction (4) showing  $k_4$  (on a logarithmic scale) against the inverse of the temperature. Previous temperature dependent studies from Table 10 are shown along with the results from this study and the new recommendation. Thick lines represent recommendations and the thin lines represent upper and lower error limits.

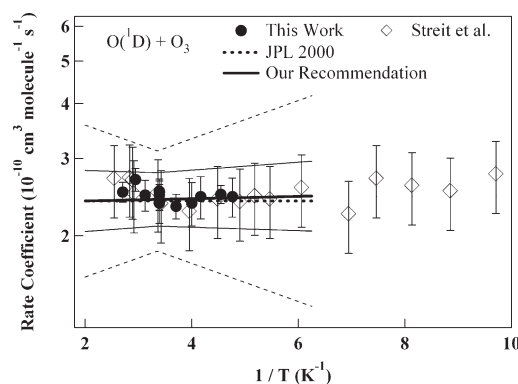


**Fig. 6** Arrhenius plot for reaction (5) showing  $k_5$  (on a logarithmic scale) against the inverse of the temperature. Previous temperature dependent studies from Table 11 are shown along with the results from this study and the new recommendation. Thick lines represent recommendations and the thin lines represent upper and lower error limits.

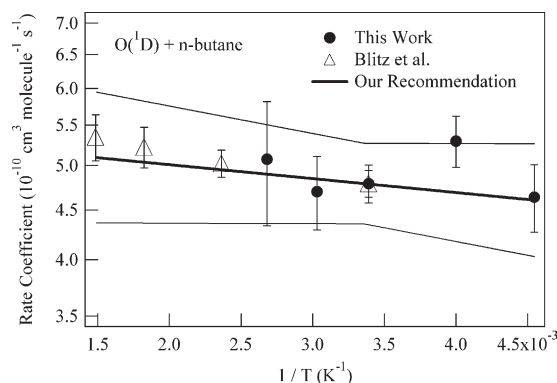


**Fig. 7** Arrhenius plot for reaction (6) showing  $k_6$  (on a logarithmic scale) against the inverse of the temperature. Previous temperature dependent studies from Table 12 are shown along with the results from this study and the new recommendation. Thick lines represent recommendations and the thin lines represent upper and lower error limits.

ratio was the result of the rate coefficient for  $O(^1D) + CO_2$  remaining essentially the same with the rate coefficient for  $O(^1D) + N_2O$  being slightly larger. Overall, we concluded that our newer rate coefficient measurements improved the uncertainty in the integrated experiments of Greenblatt and Ravishankara from roughly  $\pm 30\%$  to roughly  $\pm 20\%$ . This is the same level of uncertainty as that from the extrapolation of the uncertainties in our individual rate coefficients. We conclude that the overall uncertainty in the calculated rate of

**Table 7** Measured values of  $k_6$  at various temperatures and the experimental conditions employed for their determination

$T/K$	$P/\text{Torr}$	Flow velocity/ $\text{cm s}^{-1}$	$[\text{O}_3]/10^{13} \text{ cm}^{-3}$	Fluence/ $\text{mJ pulse}^{-1} \text{ cm}^{-2 a}$	$10^{-11}[\text{O}(^1\text{D})]_0/\text{cm}^{-3}$	$10^{-13}[\text{n-C}_4\text{H}_{10}]/\text{cm}^{-3}$	$k_6'/\text{s}^{-1}$	$10^{10}k_6/\text{cm}^3 \text{ s}^{-1}$
220	27	11.7	1.71	2.1	8.0	1.02–2.26	7070–19 500	$4.86 \pm 0.51$
220	28	11.5	1.80	2.1	8.3	0.80–2.84	6300–19 207	$4.57 \pm 0.37$
250	26	14.1	1.42	3	9.1	0.53–2.58	5880–21 900	$5.22 \pm 0.32$
295	25	17.1	1.62	2.3	8.0	0.69–2.53	9228–20 150	$4.66 \pm 0.33$
295	23	18.8	1.36	3.3	9.5	0.65–2.67	5000–20 400	$4.72 \pm 0.22$
330	25	19.3	1.48	3	7.3	0.56–2.64	6850–22 900	$4.63 \pm 0.41$
370	26	20.8	1.29	2.6	7.2	0.32–2.33	6000–19 200	$5.00 \pm 0.74$

<sup>a</sup> Laser repetition rate 4 Hz.**Table 8** Comparison of the rate coefficient for the reaction  $\text{O}(^1\text{D})$  with  $\text{O}_2$ ,  $k_2$ , obtained in this study with those from other studies

$T/K$	$k_2(298 \text{ K})^a$	$A^a$	$(E_a/R)/\text{K}$	$f(298)$	Reference
104–354	$3.65 \pm 0.7$ $4.2 \pm 0.2$ $4.0 \pm 0.6$ 4.18	$2.9 \pm 0.6$   $3.39 \pm 0.03$	$-70 \pm 15$   $-63 \pm 3$		Davidson (Streit) <i>et al.</i> , 1976 <sup>22</sup> Amimoto <i>et al.</i> , 1979 <sup>18</sup> Lee and Slinger, 1978 <sup>23</sup> Strekowski <i>et al.</i> , 2004 <sup>7</sup>
104–354	$4.1 \pm 0.3$ $4.0 \pm 1.6$	$3.1 \pm 0.3$ 3.2	$-87 \pm 30$ $-70 \pm 100$	1.2	Blitz <i>et al.</i> , 2004 <sup>2</sup> JPL, 2000 <sup>3</sup>
210–370	$3.89 \pm 0.25$ 3.95	$3.65 \pm 0.23$ 3.12	$-22 \pm 10$ $-70 \pm 10$	1.08	This work, 2004 Our Recommendation

<sup>a</sup> In units of  $10^{-11} \text{ cm}^3 \text{ molecule}^{-1} \text{ s}^{-1}$ .**Table 9** Comparison of the rate coefficient for the reaction  $\text{O}(^1\text{D})$  with  $\text{N}_2\text{O}$ ,  $k_3$ , obtained in this study with those from other studies

$T/K$	$k_3(298 \text{ K})^a$	$A^a$	$(E_a/R)/\text{K}$	$f(298)$	Reference
200–350	$1.1 \pm 0.2$ $1.2 \pm 0.1$ $1.17 \pm 0.12$ $1.07 \pm 0.08$	$1.1 \pm 0.2$   $0.97 \pm 0.10$	0		Davidson <i>et al.</i> , 1976 (&77) <sup>21</sup> Amimoto <i>et al.</i> , 1979 <sup>18</sup> Wine and Ravishankara, 1981 <sup>9</sup> Blitz <i>et al.</i> , 2004 <sup>2</sup>
200–350	$1.16 \pm 0.70$	1.16	$0 \pm 100$	1.3	JPL, 2000 <sup>3</sup>
210–370	$1.27 \pm 0.08$ 1.18	$1.17 \pm 0.20$ 1.11	$-40 \pm 50$ $-17 \pm 40$	1.10	This work, 2004 Our recommendation

<sup>a</sup> In units of  $10^{-10} \text{ cm}^3 \text{ molecule}^{-1} \text{ s}^{-1}$ .**Table 10** Comparison of the rate coefficient for the reaction  $\text{O}(^1\text{D})$  with  $\text{CO}_2$ ,  $k_4$ , obtained in this study with those from other studies

$T/K$	$k_4(298 \text{ K})^a$	$A^a$	$(E_a/R)/\text{K}$	$f(298)$	Reference
139–200	$1.01 \pm 0.2$	$1.2 \pm 0.2$	0		Davidson (Streit) <i>et al.</i> , 1976 <sup>22</sup>
200–354	$0.68 \pm 0.14$ $1.28 \pm 0.07$ $1.04 \pm 0.1$ $1.05 \pm 0.18$ $0.90 \pm 0.08$	    $1.34 \pm 1.0$	$-120 \pm 20$    $-21 \pm 2$		Davidson (Streit) <i>et al.</i> , 1976 <sup>22</sup> Amimoto <i>et al.</i> , 1979 <sup>18</sup> Wine and Ravishankara, 1981 <sup>9</sup> Shi and Barker, 1990 <sup>30</sup> Blitz <i>et al.</i> , 2004 <sup>2</sup>
200–354	$1.1 \pm 0.2$	0.74	$-120 \pm 100$	1.2	JPL, 2000 <sup>3</sup>
210–370	$1.14 \pm 0.07$ 1.15	$0.79 \pm 0.07$ 0.74	$-110 \pm 20$ $-133 \pm 40$	1.10	This work, 2004 Our Recommendation

<sup>a</sup> In units of  $10^{-10} \text{ cm}^3 \text{ molecule}^{-1} \text{ s}^{-1}$ .

stratospheric  $\text{NO}_x$  due to the reaction of  $\text{O}(^1\text{D})$  with  $\text{N}_2\text{O}$  is roughly  $\pm 20\%$  if the abundances of  $\text{N}_2\text{O}$  and  $\text{O}(^1\text{D})$  are known.

## $\text{CO}_2$

Our values for the room temperature rate coefficient and its temperature dependence are in excellent agreement with the

current recommendation. The average of the six room temperature values listed in Table 10 is  $(1.15 \pm 0.34)$ , with a range of 0.97 to 1.44, all in units of  $10^{-10} \text{ cm}^3 \text{ molecule}^{-1} \text{ s}^{-1}$ . The temperature dependence of  $k_4$  has been previously reported by Streit *et al.*<sup>22</sup> We normalized both our values of  $k_4$  and theirs at each temperature to the average value of  $k_4$  (298 K) noted above and determined new Arrhenius parameters of  $A = (7.40 \pm 0.11) \times 10^{-11} \text{ cm}^3 \text{ molecule}^{-1} \text{ s}^{-1}$  and

**Table 11** Comparison of the rate coefficient for the reaction O(<sup>1</sup>D) with O<sub>3</sub>, *k*<sub>5</sub>, obtained in this study with those from other studies

<i>T</i> /K	<i>k</i> <sub>5</sub> (298 K) <sup>a</sup>	<i>A</i> <sup>a</sup>	( <i>E</i> <sub>a</sub> / <i>R</i> )/K	<i>f</i> (298)	Reference
103–393	2.5 ± 0.1	2.4 ± 0.5	0	1.3	Gilpin <i>et al.</i> , 1971 <sup>31</sup>
	2.7 ± 0.2				Heidner and Husain, 1972 <sup>15,16</sup>
	2.4 ± 0.5				Davidson (Streit) <i>et al.</i> , 1976 <sup>22</sup>
	2.41 ± 0.11				Amimoto <i>et al.</i> , 1979 <sup>18</sup>
200–300	2.28 ± 0.23	2.3 ± 0.5	0	1.3	Wine and Ravishankara, 1981 <sup>9</sup>
	2.3 ± 0.5				Talukdar <i>et al.</i> , 1997 <sup>13</sup>
103–393	2.4 ± 0.7	2.4	0 ± 100	1.3	JPL, 2000 <sup>3</sup>
210–370	2.45 ± 0.13	2.65 ± 0.35	20 ± 40	1.15	This work, 2004
	2.42	2.37	–6 ± 15		Our Recommendation

<sup>a</sup> In units of 10<sup>–10</sup> cm<sup>3</sup> molecule<sup>–1</sup> s<sup>–1</sup>.

**Table 12** Comparison of the rate coefficient for the reaction O(<sup>1</sup>D) with n-C<sub>4</sub>H<sub>10</sub>, *k*<sub>6</sub>, obtained in this study with those from other studies

<i>T</i> /K	<i>k</i> <sub>6</sub> (298 K) <sup>a</sup>	<i>A</i> <sup>a</sup>	( <i>E</i> <sub>a</sub> / <i>R</i> )/K	<i>f</i> (298)	Reference
295–673	5.1 ± 0.2	5.45 ± 0.50	55 ± 27	1.1	Michaud <i>et al.</i> , 1974 <sup>5</sup>
	4.55 ± 0.15				Blitz <i>et al.</i> , 2004 <sup>2</sup>
220–370	4.80 ± 0.40	5.00 ± 1.55	10 ± 90	1.1	This work, 2004
	4.79	5.35	33 ± 32		Our Recommendation

<sup>a</sup> In units of 10<sup>–10</sup> cm<sup>3</sup> molecule<sup>–1</sup> s<sup>–1</sup>.

*E*<sub>a</sub>/*R* = –133 ± 40 K based on the combination of both studies. Over the range of temperatures typical of the atmosphere, using this new *E*<sub>a</sub>/*R* instead of the currently recommended value changes the rate coefficient for quenching of O(<sup>1</sup>D) by CO<sub>2</sub> by less than 10%.

### O<sub>3</sub>

O<sub>3</sub> held in dilute mixtures thermally decomposes at room temperature over the course of a month or so. The experiments done to determine *k*<sub>5</sub> were all performed with fresh O<sub>3</sub> mixtures to minimize the build-up of O<sub>2</sub>. Our room temperature value for *k*<sub>5</sub> agreed very well with all six previous determinations listed in Table 11. We measured no significant temperature dependence for reaction (5), in agreement with the two previous temperature dependent studies.<sup>13,22</sup> We normalized the temperature dependent data from the three studies to *k*<sub>5</sub>(298 K) = (2.42 ± 0.30) × 10<sup>–10</sup> cm<sup>3</sup> molecule<sup>–1</sup> s<sup>–1</sup> and calculated the following Arrhenius expression: *k*<sub>5</sub> = (2.37 ± 0.15) × 10<sup>–11</sup> × exp((6 ± 15)/*T*) cm<sup>3</sup> molecule<sup>–1</sup> s<sup>–1</sup> (2σ uncertainties).

### n-butane

Our room temperature value agreed well with the other two determinations listed in Table 12. The average of the three measurements is *k*<sub>6</sub>(298 K) = (4.95 ± 0.34) × 10<sup>–10</sup> cm<sup>3</sup> molecule<sup>–1</sup> s<sup>–1</sup>. Both of the temperature dependent studies (ours, and Blitz *et al.*) were then normalized to this value to obtain *k*<sub>6</sub> = (5.35 ± 0.56) × 10<sup>–11</sup> × exp((33 ± 32)/*T*) cm<sup>3</sup> molecule<sup>–1</sup> s<sup>–1</sup> (2σ uncertainties).

### He

As stated, the intercept of the plot of the first order rate coefficient for O(<sup>3</sup>P) rise (eqn. (III)) versus the concentration of O<sub>3</sub> in the bottom panel of Fig. 2. This intercept defines an upper limit for the rate coefficient for the reaction of O(<sup>1</sup>D) with He of <1 × 10<sup>–15</sup> cm<sup>3</sup> molecule<sup>–1</sup> s<sup>–1</sup>. This is consistent with previous determinations of this rate coefficient of <7.0 × 10<sup>–16</sup>, <3.0 × 10<sup>–15</sup>, and <3.0 × 10<sup>–13</sup> cm<sup>3</sup> molecule<sup>–1</sup> s<sup>–1</sup>

by Heidner and Husain,<sup>28</sup> Schofield,<sup>29</sup> and Shi and Barker,<sup>30</sup> respectively.

In summary, we have measured the rate coefficients for reactions (1)–(6) over a range of atmospherically relevant temperatures. In general, our results confirm current recommendations for these rates coefficients with a couple of notable exceptions. First, the rate coefficient for the quenching of O(<sup>1</sup>D) by N<sub>2</sub> has been shown to be approximately 15% faster than previously determined.<sup>6</sup> Second, we have measured a slightly smaller temperature dependence for the quenching of O(<sup>1</sup>D) by O<sub>2</sub>. For the atmospheric production rate of NO<sub>x</sub>, our individual rate coefficient measurements are slightly more precise than previous determinations, and our results improve the accuracy of the NO<sub>x</sub> production rate calculated in the integrated study of Greenblatt and Ravishankara.<sup>27</sup> Overall, our results reduce the uncertainty in the calculated NO<sub>x</sub> production rate to ±20%.

### Acknowledgements

We thank Sandra Laursen and Steve Barone for help during the initial stages of this work. We thank Paul Wine, Dwayne Heard, and their coworkers for providing us their data prior publication. This work was funded in part by NASA's Upper Atmosphere Research Project and NASA's Earth System Science doctoral Fellowship to EJD.

### References

- R. P. Wayne, *Chemistry of Atmospheres*, 2nd edn., Oxford University Press, New York, 1991.
- M. A. Blitz, T. J. Dillon, D. E. Heard, M. J. Pilling and I. D. Trought, *Phys. Chem. Chem. Phys.*, 2004, **6**, DOI: 10.1039/b400283k.
- S. P. Sander and D. M. Golden, *et al.*, *Chemical kinetics and photochemical data for use in stratospheric modeling*, Jet Propulsion Laboratory, California Institute of Technology, JPL Publication 00-3, Evaluation No. 13, 2000.
- R. Atkinson, D. L. Baulch, R. A. Cox, J. Crowley, R. F. Hampson, M. E. Jenkins, J. A. Kerr, M. J. Rossi and J. Troe, IUPAC Subcommittee for Gas Kinetic Data Evaluation, Evaluated Kinetic Data, <http://www.iupac-kinetic.ch.cam.ac.uk/>.
- P. Michaud, G. Paraskevopoulos and R. J. Cvetanovic, *J. Phys. Chem.*, 1974, **78**, 1457–1461.

- 6 A. R. Ravishankara, E. J. Dunlea, M. A. Blitz, T. J. Dillon, D. E. Heard, M. J. Pilling, R. E. Strekowski, J. M. Nicovich and P. H. Wine, *Geophys. Res. Lett.*, 2002, **29**, DOI: 10.1029/2002GL014850.
- 7 R. S. Strekowski, J. M. Nicovich and P. Wine, *Phys. Chem. Chem. Phys.*, 2004, **6**, DOI: 10.1039/b400243a.
- 8 R. F. Warren and A. R. Ravishankara, *Int. J. Chem. Kinet.*, 1993, **25**, 833–844.
- 9 P. H. Wine and A. R. Ravishankara, *Chem. Phys. Lett.*, 1981, **77**, 103–109.
- 10 F. C. Fehsenfeld, K. M. Evenson and H. P. Broida, *Microwave discharge cavities operating at 2450 MHz*, National Bureau of Standards Document 8701, NBS, Gaithersburg, MD, 1964.
- 11 F. C. Fehsenfeld, K. M. Evenson and H. P. Broida, *Rev. Sci. Instrum.*, 1965, **36**, 294–298.
- 12 Y. Matsumi, F. J. Comes, G. Hancock, A. Hofzumahaus, A. J. Hynes, M. Kawasaki and A. R. Ravishankara, *J. Geophys. Res.*, 2002, **107**, DOI: 10.1029/2001JD000510.
- 13 R. K. Talukdar, C. A. Longfellow, M. K. Gilles and A. R. Ravishankara, *Geophys. Res. Lett.*, 1998, **25**, 143–146.
- 14 E. J. Dunlea, PhD Thesis, University of Colorado at Boulder, 2002.
- 15 R. F. I. Heidner and D. Husain, *Int. J. Chem. Kinet.*, 1973, **5**, 819–831.
- 16 R. F. I. Heidner, III, D. Husain and J. R. Wiesenfeld, *J. Chem. Soc. Faraday Trans. 2*, 1973, **69**, 927–938.
- 17 S. T. Amimoto, A. P. Force and J. R. Wiesenfeld, *Chem. Phys. Lett.*, 1978, **60**, 40–43.
- 18 S. T. Amimoto, A. P. Force, R. G. Gulotty, Jr. and J. R. Wiesenfeld, *J. Chem. Phys.*, 1979, **71**, 3640–3647.
- 19 S. T. Amimoto and J. R. Wiesenfeld, *J. Chem. Phys.*, 1980, **72**, 3899–3903.
- 20 J. A. Davidson, C. M. Sadowski, H. I. Schiff, G. E. Streit, C. J. Howard, D. A. Jennings and A. L. Schmeltekopf, *J. Chem. Phys.*, 1976, **64**, 57–62.
- 21 J. A. Davidson and H. I. Schiff, *J. Chem. Phys.*, 1977, **67**, 5021–5025.
- 22 G. E. Streit, C. J. Howard, A. L. Schmeltekopf, J. A. Davidson and H. I. Schiff, *J. Phys. Chem.*, 1976, **65**, 4761–4764.
- 23 L. C. Lee and T. G. Slanger, *J. Chem. Phys.*, 1978, **69**, 4053–4060.
- 24 L. C. Lee and T. G. Slanger, *Geophys. Res. Lett.*, 1979, **6**, 165–166.
- 25 P. H. Wine and A. R. Ravishankara, *Chem. Phys.*, 1982, **69**, 365–373.
- 26 P. H. Wine and A. R. Ravishankara, *Chem. Phys. Lett.*, 1983, **96**, 129–132.
- 27 G. D. Greenblatt and A. R. Ravishankara, *J. Geophys. Res.*, 1990, **95**, 3539–3547.
- 28 R. F. I. Heidner and D. Husain, *Int. J. Chem. Kinet.*, 1974, **6**, 77.
- 29 K. Schofield, *J. Photochem.*, 1978, **9**, 55, and references therein.
- 30 J. Shi and J. R. Barker, *Int. J. Chem. Kinet.*, 1990, **20**, 1283–1301.
- 31 R. Gilpin, H. I. Schiff and K. H. Welge, *J. Chem. Phys.*, 1971, **55**, 1087–1093.